Numerical Results for the Symmetrical Condensed TLM Node

ROGER ALLEN, ALAK MALLIK, AND PETER JOHNS

Abstract—**Numerical calculations have been made in order to test the accuracy of the recently derived three-dimensional symmetrical condensed TLM node for electromagnetics. Demonstrations of its use in these areas are given. Analysis of dispersion characteristics shows that the velocity error bound for the new symmetrical condensed node is likely to be less than that for the expanded node. Predictions of the surface currents on an F-111 aircraft due to the scattering of an incident plane wave are in good agreement with other computed codes and measurements. Lastly, the introduction of stubs into the scattering node allows generalization to a cylindrical mesh, which is tested by finding coaxial cavity modes.**

I. Introduction

THE THEORETICAL development of the new symmetrical condensed TLM node for the solution of electromagnetic problems is described in [1]. The purpose of this paper is to present numerical results to test the accuracy of the node and to demonstrate its use.

II. Propagation Assessment in Simple Cavities

It would require extensive detailed analysis of the symmetrical condensed node to obtain general dispersion characteristics similar to those obtained for the expanded node in [2]. This work has not yet been done and so numerical results are used here to assess this error. The velocity of waves is observed in the three principal propagation directions in the mesh by obtaining the resonant frequency of modes in rectangular cavities and comparing them with analytical results.

In [1] it was possible to predict the characteristics for two different directions of propagation on the three-dimensional symmetrical-condensed-node mesh. If ϕ_x, ϕ_y, and ϕ_z are the angles between the direction of propagation and the x, y, and z axes, then for $\phi_x = 0$ and $\phi_y = \phi_z = \pi/2$ (i.e., propagation in the direction of the x axis) the mesh was shown to be dispersionless. for $\phi_x = \phi_z = \pi/4$ and $\phi_y = \pi/2$, it was seen that the mesh behaved like two separate two-dimensional series meshes carrying waves traveling in the coordinate directions.

These propagation characteristics are tested by taking a two-dimensional slice out of the three-dimensional symmetrical-condensed-node mesh and using it to model the cross section of a $10\,\Delta l \times 10\,\Delta l$ square waveguide (where Δl is the distance between nodes in the mesh). Results for the cutoff frequencies for TM modes are compared with results already obtained for a two-dimensional shunt-node mesh in [3]. The comparison is shown in Table I and results are expressed in terms of $\Delta l/\lambda$, where λ is the free-space wavelength in a medium of $\epsilon_r = \mu_r = 1$ (in contrast to a medium of $\epsilon_r = 2$ and $\mu_r = 1$ in [3]). In all cases, sufficient timesteps are made to keep the truncation error less than 0.2 percent.

Highly accurate results are obtained for the two-dimensional mesh for TM_{nn}-type modes. This is because waves are traveling at $\phi_x = \phi_z = \pi/4$ on the mesh and propagation in this direction is dispersionless for the two-dimensional mesh. In contrast, the results for TM_{nn} modes for the slice in the three-dimensional mesh are less accurate because dispersion now takes place. Conversely, TM_{1n} modes are highly accurate for the three-dimensional mesh where the propagation direction is near to a coordinate direction, where this mesh is dispersionless.

These results can be confirmed in detail by propagation analysis. However, in more general problems waves do not travel in just one direction through the mesh, and it is convenient to use a velocity error bound. On the two-dimensional mesh, the dispersion is most pronounced in the $\phi_x = 0$ direction, where the ratio of wave velocity v on the network to the free-space velocity c is given by [2]

$$\frac{v}{c} = \pi \frac{\Delta l}{\lambda} \frac{1}{\sin^{-1}\left[\sqrt{2}\sin\left(\frac{\pi}{\sqrt{2}}\frac{\Delta l}{\lambda}\right)\right]}. \tag{1}$$

This formula is used to calculate the bound for the two-dimensional mesh in Table II.

On the two-dimensional slice in the three-dimensional mesh, it is assumed that the worst dispersion is for propagation in the $\phi_x = \pi/4$ direction. It is indicated in [1] that propagation is now identical to $\phi_x = 0$ on a true two-dimensional mesh but with wavelengths increased by a factor of $\sqrt{2}$. In this case, the bound is given by

$$\frac{v}{c} = \frac{\pi}{\sqrt{2}} \frac{\Delta l}{\lambda} \frac{1}{\sin^{-1}\left[\sqrt{2}\sin\left(\frac{\pi}{2}\frac{\Delta l}{\lambda}\right)\right]}. \tag{2}$$

This bound is used for the three-dimensional slice in Table II.

Manuscript received March 20, 1986; revised November 24, 1986.

R. Allen and A. Mallik are with Kimberley Communications Consultants Ltd., Nottingham, England NG1 6EP.

P. Johns is with Kimberley Communications Consultants Ltd., Nottingham, and with the Department of Electrical and Electronic Engineering, University of Nottingham, Nottingham, England NG7 2RD.

IEEE Log Number 8613285.

0018-9480/87/0400-0378$01.00 ©1987 IEEE

TABLE I
MODES IN A 10 $\Delta l \times 10\ \Delta l$ SQUARE TWO-DIMENSIONAL CAVITY

MODE	CUT-OFF FREQUENCIES $\Delta\ell/\lambda$				
	ANALYTICAL	2-d MESH	ERROR %	3-d SLICE	ERROR %
TM_{11}	0.0707	0.0707	0.0	0.0706	0.1
TM_{13}	0.1581	0.1561	1.3	0.1578	0.2
TM_{33}	0.2121	0.2118	0.1	0.2080	1.9
TM_{15}	0.2550	0.2418	5.2	0.2540	0.4

TABLE II
VELOCITY ERROR BOUNDS FOR MODES IN TABLE I

MODE	$\Delta\ell/\lambda$ ANALYTICAL	VELOCITY REDUCTION BOUND %	
		2-d MESH	3-d SLICE
TM_{11}	0.0707	0.4	0.2
TM_{13}	0.1581	2.3	1.1
TM_{33}	0.2121	4.6	2.0
TM_{15}	0.2550	7.6	3.1

The results of Table I for the three-dimensional slice are all within the bounds and are close to the bound in the case of TM_{nn}-type modes. These results tend to confirm the predictions made in [1].

The most interesting result, however, is that for two-dimensional problems, a two-dimensional slice taken out of a symmetrical-condensed-node three-dimensional mesh is more accurate in terms of velocity error than a true two-dimensional shunt- or series-node mesh.

Results for three-dimensional cavities are given in Table III, where the $6\times4\times3$ cavity results are compared with those obtained by the expanded-node mesh in [4]. The increased accuracy for the condensed node is to be expected for TM_{mno}-type modes since these again involve two-dimensional propagation and the true two-dimensional meshes are more accurate than two-dimensional propagation on the expanded mesh [2].

The velocity error for the expanded node mesh is given by [2]

$$\sin^2\left[\frac{\pi c\Delta l}{\lambda v}\cos\phi_x\right]+\sin^2\left[\frac{\pi c\Delta l}{\lambda v}\cos\phi_y\right]+\sin^2\left[\frac{\pi c\Delta l}{\lambda v}\cos\phi_z\right]=4\sin^2\left[\frac{\pi\Delta l}{2\lambda}\right]. \quad (3)$$

Thus, for waves propagating in the $\phi_x=\phi_y=\phi_z$ direction, the error is given by

$$\frac{v}{c}=\frac{\pi}{\sqrt{3}}\frac{\Delta l}{\lambda}\frac{1}{\sin^{-1}\left[\frac{2}{\sqrt{3}}\sin\left(\frac{\pi}{2}\frac{\Delta l}{\lambda}\right)\right]}. \quad (4)$$

TABLE III
MODES IN THREE-DIMENSIONAL RECTANGULAR CAVITIES

CAVITY DIMENSIONS $\Delta\ell$	MODE	CONDENSED NODE $\Delta\ell/\lambda$		EXPANDED NODE $\Delta\ell/\lambda$		
		FREQUENCY	ERROR %	FREQUENCY	ERROR %	BOUND %
6 x 4 x 3	TM_{110}	0.1490	0.8	0.1482	1.3	
6 x 4 x 3	TM_{210}	0.2048	1.5	0.2040	2.1	
10 x 10 x 10	TM_{111}	0.0863	0.4		0.1	0.9
10 x 10 x 10	TM_{333}	0.2576	0.8		1.0	12.3

The analytical result for the TM_{111} mode in a $10\times10\times10$ waveguide is

$$\frac{\Delta l}{\lambda}=\frac{\sqrt{3}}{20}$$

and substituting this into (4) gives

$$\frac{c}{v}=1.00104$$

showing the good accuracy for propagation on the expanded-node mesh in this direction.

The results for the TM_{111} mode in Table III clearly show that the symmetrical condensed node is not as accurate in this direction.

The velocity characteristics for the expanded node in other directions are

$$\frac{v}{c}=\frac{\pi}{\sqrt{2}}\frac{\Delta l}{\lambda}\frac{1}{\sin^{-1}\left[\sqrt{2}\sin\left(\frac{\pi}{2}\frac{\Delta l}{\lambda}\right)\right]}$$

$$\phi_x=\phi_y=\pi/4 \quad \phi_2=\pi/2 \quad (5)$$

and

$$\frac{v}{c}=\pi\frac{\Delta l}{\lambda}\frac{1}{\sin^{-1}\left[2\sin\left(\frac{\pi}{2}\frac{\Delta l}{\lambda}\right)\right]}$$

$$\phi_x=0 \quad x_y=\phi_z=\pi/2 \quad (6)$$

giving velocity errors of 0.3 percent and 0.9 percent, respectively, for $\Delta l/\lambda=\sqrt{3}/20$. The latter result represents the direction of worst error and therefore forms the bound in Table III.

Results for the TM_{333} in Table III show that a similar comparison can be made at a higher frequency in the same direction of propagation.

If it is assumed that the $\phi_x=\phi_y=\phi_z$ direction has the worst dispersion characteristics in the symmetrical condensed node, then it can be concluded that this is better than the worst dispersion in the expanded-node case.

The conclusion for three-dimensional propagation, if the above assumption is correct, is that the overall accuracy of the symmetrical condensed node, in terms of velocity error, is better than the expanded node.

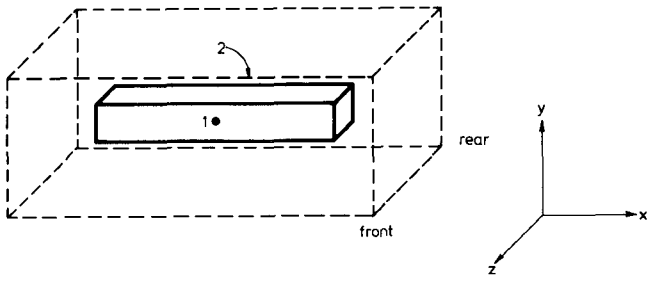

Fig. 1. Geometry of test cylinder for scattering test. Cylinder dimensions: 19 m×3 m×3 m. Space box dimensions: 29 m×11 m×11 m. Excitation, E_x plane wave at front or back.

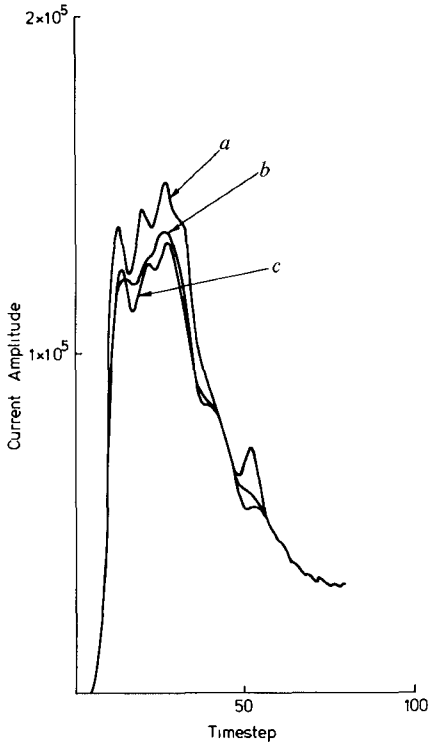

Fig. 2. Results for scattering for test cylinder. Curve *a*: asymmetrical condensed node; excitation from front, output point 1. Curve *b*: symmetrical condensed node; excitation from front, output point 1, or excitation from rear, output point 2. Curve *c*: asymmetrical condensed node; excitation from rear, output point 2.

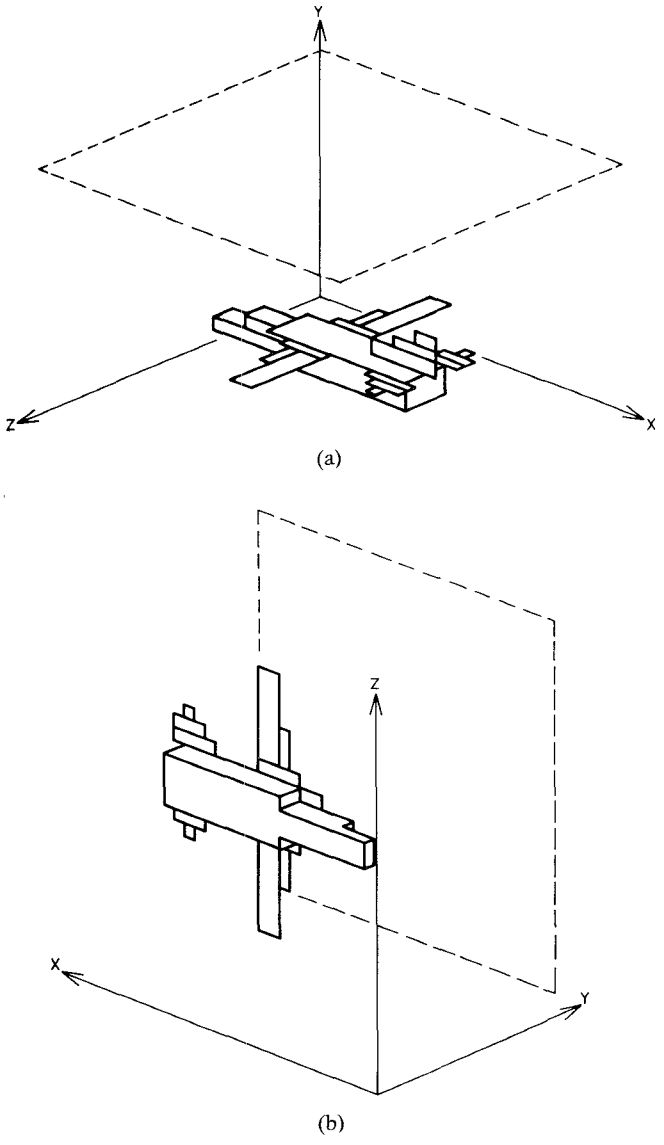

Fig. 3. Geometry of F-111 aircraft for scattering test. (a) View from above. (b) View from underneath.

III. Time-Domain Scattering

The condensation of the expanded-node mesh into an asymmetrical or point node [5], [6] represents a significant improvement in the modeling technique for reasons given in [1]. The node, however, does have asymmetry in that when viewed in one direction a shunt connection is first seen, while when viewed in the opposite direction a series connection is first seen. In many situations, this asymmetry seems to have little effect. In cavity resonance problems, for example, it is likely that any apparent shift in the position of one boundary is compensated by an equivalent shift in another. In scattering problems, however, the asymmetry can be more apparent, and this is demonstrated by the following simple scattering problem.

Fig. 1 shows a conducting cylinder contained in a box of space with absorbing boundaries. A plane of E field excites the problem and this can be either at the "front" or the "rear" of the cylinder. The geometry is perfectly symmetrical and so there should be no difference between the two excitations. However, the asymmetrical-condensed-node mesh does appear different in the two directions and so numerically there is a difference. Fig. 2 shows results for the x-directed surface current at output point 1 for excitation from the front compared with the output at point 2 for excitation from the rear. In both cases, the excitation function was

$$f(t) = E_0\left[\exp\left(-t/\tau_f\right) - \exp\left(-t/\tau_r\right)\right] \qquad (7)$$

where $E_0 = 5.92\times10^4$, $\tau_f = 245\times10^{-9}$ s, and $\tau_r = 2.85\times10^{-9}$ s.

Fig. 2 also shows the result for the symmetrical condensed node, and it is pleasing to note that it lies between the two results for the asymmetrical mesh. The symmetrical node gives precisely the same result for both front and rear excitation, of course.

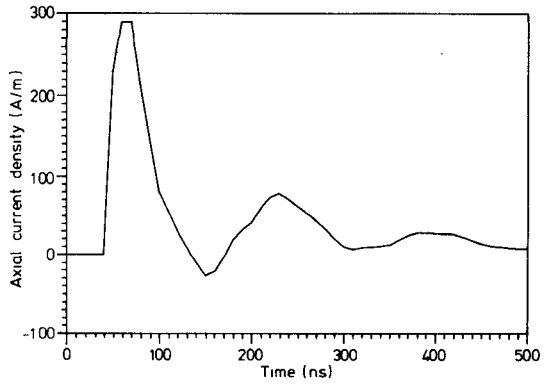

Fig. 4. Scattering result for F-111 aircraft.

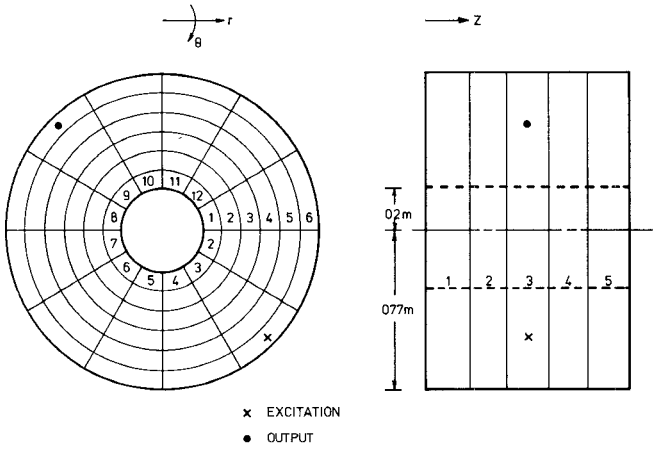

Fig. 5. Coaxial cavity geometry.

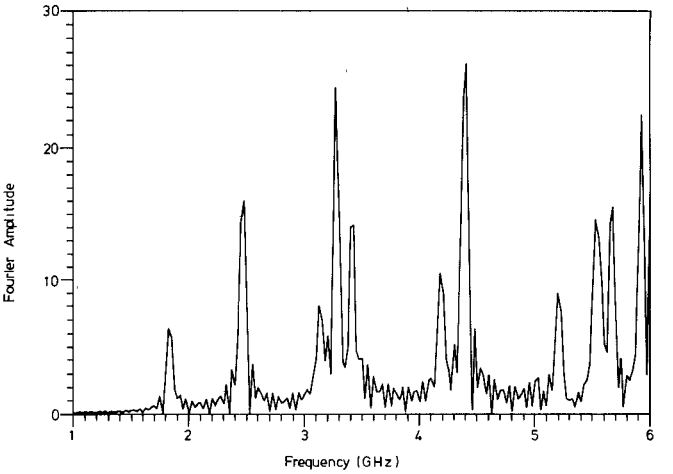

Fig. 6. Frequency-domain result for coaxial cavity.

TABLE IV
MODES IN A COAXIAL CAVITY

MODE (τ, θ, z)	FREQUENCY (GHz)
101	3.16
111	1.81
121	2.39
201	5.56
211	3.46
221	4.20
102	4.09
112	3.16
122	3.53
202	6.14
212	4.32
222	4.94

The geometry for calculating the electromagnetic pulse (EMP) response of an F-111 aircraft when illuminated with a plane wave with E field along the fuselage is shown in Fig. 3(a) and (b). The data preparation for this problem exploits the regularity of the symmetrical-condensed-node mesh. It was generated by a simple three-dimensional modeler package in which the primitive building shape is a rectangular sheet, the surface of the aircraft and the excitation being made up of these primitives. The problem is chosen because it represents a reasonably complicated scattering problem for which there are measured results and for which results have been obtained by other numerical methods. The axial current density on the top face of the fuselage obtained by the symmetrical-condensed-node mesh is shown in Fig. 4, and this result shows good agreement with measurements and with results obtained by the finite-difference code THREDE [7]. The result also agrees with that obtained by Garthwaite, Armour, and Moore using wire grid modeling [8].

The workspace in this scattering problem was surrounded by absorbing boundaries formed by setting the reflection coefficient for incident pulses to zero.

IV. The Use of Stubs in a Cylindrical Mesh

TLM is not restricted to a regular Cartesian mesh; it can be used with graded meshes and general orthogonal meshes. The cylindrical mesh provides an excellent test for the stubs since it uses both additional capacitance and additional inductance at each node.

The test problem chosen is the coaxial cavity shown in Fig. 5 using a cylindrical mesh for r, θ, z of size $6 \times 12 \times 5$. The technique used for the varying size of elements is similar to that used in [9] and [10]. In particular, the method used here employs link lines between the nodes, all with characteristic impedance equal to the impedance of free space. The network is then scanned to choose a timestep such that, for each element, inductance and capacitance have to be added (rather than subtracted) to obtain the analytical inductance and capacitance of the element. This inductance and capacitance are then added to the nodes using the various stubs. In this way, the node with stubs described in [1] can be tested.

The timestep used was 8.39×10^{-12} s, and 2000 timesteps were taken. The H_z field was excited at the single point (6,3,3), and the output was also the H_z field at the point (6,9,3). This excitation and output were chosen to eliminate TEM modes. The result for the Fourier trans-

form of the time-domain waveform at the output point is shown in Fig. 6. The resonances of the various modes can be compared with Table IV, which gives the analytical results.

V. Conclusions

The dispersion characteristics predicted in [1] have been confirmed in this paper, and the results also show that the velocity error bound for the symmetrical condensed node is likely to be less than for the expanded node.

The accuracy of the symmetrical condensed node approach in time-domain scattering problems has also been checked by comparisons with results obtained using the well-established asymmetrical condensed TLM node, the finite-difference and moment methods, and also with measurements. In the case of the comparison with the asymmetrical node, the results for the symmetrical node fell between the perturbations caused by asymmetry.

The modification to the node scattering matrix by the addition of stubs has also been checked by calculating modes in a coaxial cavity on a cylindrical mesh.

This paper therefore substantiates the theory of the symmetrical condensed node given in [1] and demonstrates the use of this significant development in TLM for electromagnetics.

References

[1] P. B. Johns, "A symmetrical condensed node for the TLM method," pp. 370–377, this issue.

[2] C. R. Brewitt-Taylor and P. B. Johns, "On the construction and numerical solution of transmission-line and lumped network models of Maxwell's equations," *Int. J. Num. Methods Eng.*, vol. 15, pp. 13–30, 1980.

[3] P. B. Johns, "Application of the transmission-line matrix method to homogeneous waveguides of arbitrary cross-section," *Proc. Inst. Elec. Eng.*, vol. 119, no. 8, pp. 1086–1091, Aug. 1972.

[4] S. Akhtarzad and P. B. Johns, "The solution of Maxwell's equations in three space dimensions and time by the TLM method of numerical analysis," *Proc. Inst. Elec. Eng.*, vol. 122, no. 12, pp. 1344–1348, Dec. 1975.

[5] P. Saguet and S. Tedjini, "Methode des lignes de transmission en trois dimensions: modification du processus de simulation," *Ann. Telecommun.*, vol. 40, nos. 3–4, pp. 1–8, Mar.–Apr. 1985.

[6] A. Amer, "The condensed node TLM method and its application to transmission in power systems," Ph.D thesis, University of Nottingham, U.K., 1980.

[7] R. Holland, "THREDE: A free-field EMP coupling and scattering code," Mission Research Corp., Albuquerque, NM. Reference AMRC-R-85, 1977.

[8] J. Moore and R. Pizer, *Moment in Electromagnetics*. Letchworth, Hertfordshire, U.K.: Research Studies Press, 1984, ch. 8.

[9] D. A. Al-Mukhtar and J. E. Sitch "Transmission-line matrix method with irregularly graded space," *Proc. Inst. Elec. Eng.*, vol. 128, pt. H, no. 6, Dec. 1981.

[10] P. Saguet, "Le maillage parallelipipedique et le changement de maille dans la methode TLM en 3 dimensions," *Electron. Lett.*, vol. 20, no. 5, pp. 222–224, Mar. 1, 1984.

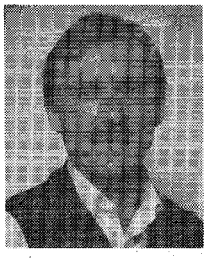

Roger Allen gained the B.Sc. and Ph.D. degrees in physics from the University of London in 1973 and 1977, respectively.

In 1977, he moved to the EEC Joint Research Centre at Karlsruhe, West Germany, where he worked on the computation of electronic structures in actinide compounds. Dr. Allen has also been involved in optical fiber beam propagation studies at Nottingham University. He is currently employed by Kimberley Communications Consultants Ltd. at Nottingham (U.K.), where his work chiefly involves the development and application of the TLM technique to problems in the design of microwave devices.

Alak Mallik was born in 1950 and obtained the Ph.D. degree in mathematics from Nottingham University (U.K.) in 1977.

From 1977 to 1980, he taught mathematics at the University of Port Harcourt, in Nigeria. On returning to the U.K. in 1981, he worked as a postdoctoral assistant to P. B. Johns in the Department of Electrical and Electronic Engineering at Nottingham University. His work was concerned with the application of the TLM method to heat diffusion in turbine disks. Since 1982, he has been with Kimberley Communications Consultants Ltd., working mostly on the simulation of electromagnetic penetration due to EMP and lightning.

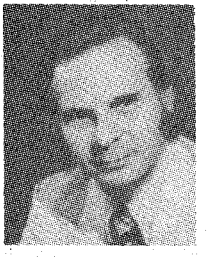

Peter B. Johns was born in Newport, Wales, in 1938. He received the B.Sc.(eng.) degree in electrical engineering and the M.Sc. degree in physics from London University, England, in 1964 and 1966, respectively and the Ph.D. degree from Nottingham University, England, in 1973.

From 1964 to 1967, he was with British Telecom Research Laboratories at Dollis Hill, London, where he worked on interference problems associated with satellite communication systems. In 1967, he was appointed Lecturer in the Department of Electrical and Electronic Engineering, University of Nottingham, and he is now Professor of Information Systems and Head of Department. He was a visiting Research Associate at the University of Manitoba in 1975/76.

Dr. Johns has originated and developed the modeling procedure TLM for computer simulation of electromagnetic waves, diffusion processes, and network analysis. He has published many papers on the subject, and in 1976 he won the Electronics Division Premium of the Institution of Electrical Engineers. He is managing Director of a small company set up in Nottingham to provide a numerical modeling service for industry. The electromagnetic applications of TLM presently include the areas of EMP/EMC and microwave tube design.